Metallurgy and Foundry Engineering – Vol. 45, 2019, No. 2, pp. 43–50
https://doi.org/10.7494/mafe.2019.45.2.43

Piotr Noga, Maria Richert, Marek Stanisław Węglowski

The influence of welding method on microstructure and mechanical properties of aluminum alloys joints

Wpływ metody spawania na mikrostrukturę i właściwości mechaniczne złączy ze stopów aluminium

Abstract
Rapid technological progress in recent years has led to an intensified interest in alternative methods of joining metals. Today's industry is constantly demanding new joining processes, which enable high-quality welded joints in a wide range of thicknesses of combined materials at low production cost. There are at least several dozen welding methods currently available. The selection of the process depends on the type of welded materials, acceptable heat input, as well as future working conditions. The paper presents the results of the microstructural examination and mechanical properties of joints of the aluminum alloy for plastic working such as EN AW-6082. The paper presents the results of microstructural observations and mechanical properties of EN AW-6082 aluminum alloy. Methods used for joining were successively TIG (welding with a non-consumable electrode in a shield of inert gases), MIG (welding with a consumable electrode in a shield of inert gases), EBW (electron beam welding) along with FSW (friction stir welding method). TIG (welding with a non-consumable electrode in a shield of inert gases), MIG (welding with a consumable electrode in a shield of inert gases), EBW (electron beam welding) along with FSW (friction stir welding method) were used as joining techniques.

Keywords: Aluminum alloys welding, TIG, MIG, EBW, FSW

Streszczenie
Współczesny przemysł wymaga opracowania i udoskonalania metod, które umożliwiają uzyskanie wysokiej jakości połączeń w szerokim zakresie grubości łączonych materiałów oraz obniżenie kosztu produkcji. Istnieje kilkadziesiąt metod spawania. Proces ten trzeba dostosować do rodzaju spajanych materiałów, dostępnych źródeł energii, a także do przyszłych warunków pracy urządzeń. W pracy przedstawiono wyniki badań łączenia najpopularniejszego stopu do przeróbki plastycznej, jakim jest stop EN AW-6082. Metodami wykorzystanymi do łączenia były zarówno najbardziej popularne techniki spawania: TIG (spawanie elektrodą nietopliwą w osłonie gazów obojętnych),

Piotr Noga: AGH University of Science and Technology, Faculty of Non-Ferrous Metals, Krakow, Poland; **Maria Richert:** AGH University of Science and Technology, Faculty of Management, Krakow, Poland; **Marek Stanisław Węglowski:** Lukasiewicz Research Network- Institute of Welding Gliwice, Poland; pionoga@agh.edu.pl

MIG (spawanie elektrodą topliwą w osłonie gazów obojętnych), metoda wysokoenergetyczna EBW (spawanie wiązką elektronową), jak również metoda zgrzewania tarciowego z mieszaniem materiały zgrzeiny – FSW.

Słowa kluczowe: spawanie stopów aluminium, TIG, MIG, FSW, EBW

1. Introduction

The development of the automotive and aerospace industries in tandem with a growing demand for light and high-strength structural components has compelled the search for new materials with enhanced mechanical properties. An effective method to improve these properties in metals and alloys is grain refinement which can be achieved through application of advanced techniques such as rapid solidification (RS) or mechanical alloying of metallic powders [1–4]. Due to plastic deformation susceptibility, high strength and good corrosion resistance 6xxx series (Al-Si-Mg) aluminum alloys have found a universal application in industries such as the automotive (elements of air conditioning systems or load-bearing elements of heavy vehicles) or shipbuilding industries [5]. Among all 6xxx series alloys, 6082 has been developed relatively recently (officially registered in 1972 [6]). Due to its high mechanical properties, it often replaces the much older 6061 alloy in many applications [7]. The alloy microstructure is stabilized by the addition of manganese, which results in enhanced mechanical properties. In addition, heat treatment for T6 or T651 condition double the strength and improves machinability [8–11]. EN AW-6082 is a weldable alloy, but some problems occur with the properties of its welded joints. In order to solve these difficulties, various fillers are used depending on the type of joined materials. In the case of welding two elements from 6082 alloy, filler materials based on the 5xxx series are usually used [12]. In the literature, a large number of references related to the 6082 alloy combined with FSW and LBW methods can be found, often in comparison with traditional welding methods, such as MIG and TIG. However, there is no comprehensive comparison of the properties of sheet metal joints from this alloy in relation to modern welding methods.

2. Experiment

For examination purposes, sheets of 6082 aluminum alloy were used with a dimensions of $2000 \times 1000 \times 6.35$ mm. The delivered sheet was solution heat-treated and artificially aged to T6 condition. The chemical composition of the aluminum alloy on the basis of the supplier certificate is shown in Table 1. The filler material in the MIG and TIG methods was 5049 aluminum alloy (Tab. 1). For both MIG and TIG, argon was used as the protective gas. Samples for joining tests had dimensions of 150×300 mm. The welding process was carried out along the edge in parallel to the rolling direction. In tests, four different joining processes were used: MIG (welding current 150 A, arc voltage 18.5 V, welding

speed 350 mm/min), TIG (welding current 178 A, arc voltage 13.6 V, welding speed 130 mm/min), electron beam welding EBW (welding current 0.0187 A, accelerating voltage 120 kV, welding speed 1600 mm/min, beam power 30 kW) and friction stir welding – FSW (welding speed 355 mm/min, rotational speed of the tool 710 rpm). Microstructure analysis with a use of scanning electron microscope (HITACHI SU-70) was performed on samples taken from joint cross-sections transverse to the welding direction. Mechanical properties were determined based on uniaxial tensile tests and hardness measurements.

Table 1 .Chemical composition of AA6082 and AA5049 acc. to supplier certificate

Element	Si	Fe	Cu	Mn	Mg	Cr	Zn	Ti	Another	Al
6082 wt. %	1.0	0.3	0.05	0.67	0.8	0.06	0.07	0.07	0.05	balance
5049 wt. %	0.40	0.50	0.10	0.8	2.2	0.30	0.2	0.1	–	balance

3. Results and discussion

Figure 1 shows the microstructure of the supersaturated and artificially aged 6082 alloy. The average grain size, measured by the planimetric method, is 92 μm. Microstructure observations revealed two types of intermetallic phases represented by dark precipitates containing magnesium and silicon and bright particles enriched with aluminum, iron, manganese and silicon (Tab. 2).

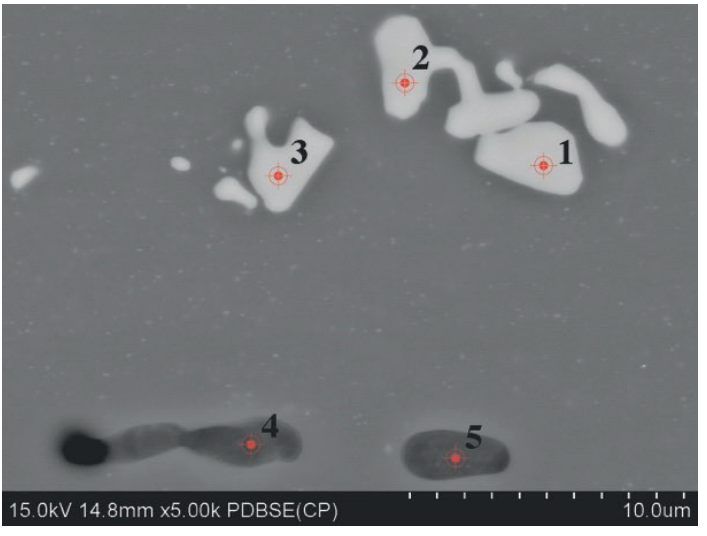

Fig. 1. Microstructure of the AA 6082 alloy

Table 2. Results of SEM/EDS chemical analysis of AA6082 alloy performed in the areas marked in Figure 1

% wt.	Mg	Al	Si	Mn	Fe
1	–	61.2	8.9	11.9	18.0
2	–	62.0	8.9	12.4	16.7
3	–	62.2	9.4	14.0	14.4
4	36.7	43.9	18.9	0.2	0.3
5	14.4	73.3	12.1	0.2	–

Based on the SEM/EDS chemical analysis and the literature data [13–15], one can conclude that the light particles are typical for the Al(Fe,Mn)Si intermetallic phases. Depending on the chemical composition, these phases have different stoichiometric composition e.g. Al_9Mn_3Si, Al_5FeSi and Al(Fe,Mn)Si. They can also be characterized by a different morphology such as columnar structure, a polyhedral, and so-called "Chinese writing". Dark precipitations rich in Mg and Si (Fig. 1, Tab. 2) are recognized as the Mg_2Si phases, the presence of which have been confirmed in various scientific research papers [16, 17].

Figure 2 presents the microstructure of welded joints obtained by various welding methods/techniques. Depending on the method and amount of heat input in the welding process, the welds differ in shape and size. Figure 2a presents the microstructure of the welded joint obtained with the MIG method. Observations have shown that the heat affected zone (HAZ) on both sides of the joint area has an average width of 2.55 mm, whereas the weld surface in the cross-section is 67.6 mm^2. The weld microstructure (Fig. 2a) is characterized by a cast microstructure with intermetallic precipitates present in the interdendritic areas. Figure 2b shows the microstructure of the welded joint obtained with the TIG method. The obtained weld shape is regular and symmetrical, with an area of 61 mm^2, while the average width of the HAZ is below 1.89 mm. At the center area of the weld (Fig. 2b), a dendritic microstructure with a eutectic mixture distributed along the grain boundaries is often associated with the particles of phases containing Al, Fe, Mn and Si. A typical microstructure of an electron beam welded 6082 alloy is shown in Figure 2c. In comparison to welded joints using the MIG and TIG methods, the weld in the EBW has the smallest surface area of 9.81 um^2 as well as the smallest average width of the HAZ – below 1 mm. The SEM studies (Fig. 2c) indicate that precipitates were significantly reduced in size with comparison to the parent material (Fig. 2a). Both the morphology and distribution of iron rich phases, represented by white particles, are differentiated depending on the area of examination. The microstructure of FSW joint is shown in Figure 2d. Detailed joint examinations revealed a lack of any welding imperfections. The enlarged area in the figure represents the microstructure of the weld nugget. In terms of the microstructure, this area is homogenous and consists of both recrystallized grains, with an average size of 9 μm and fine Al(FeSi)Mn particles fragmented during the welding process.

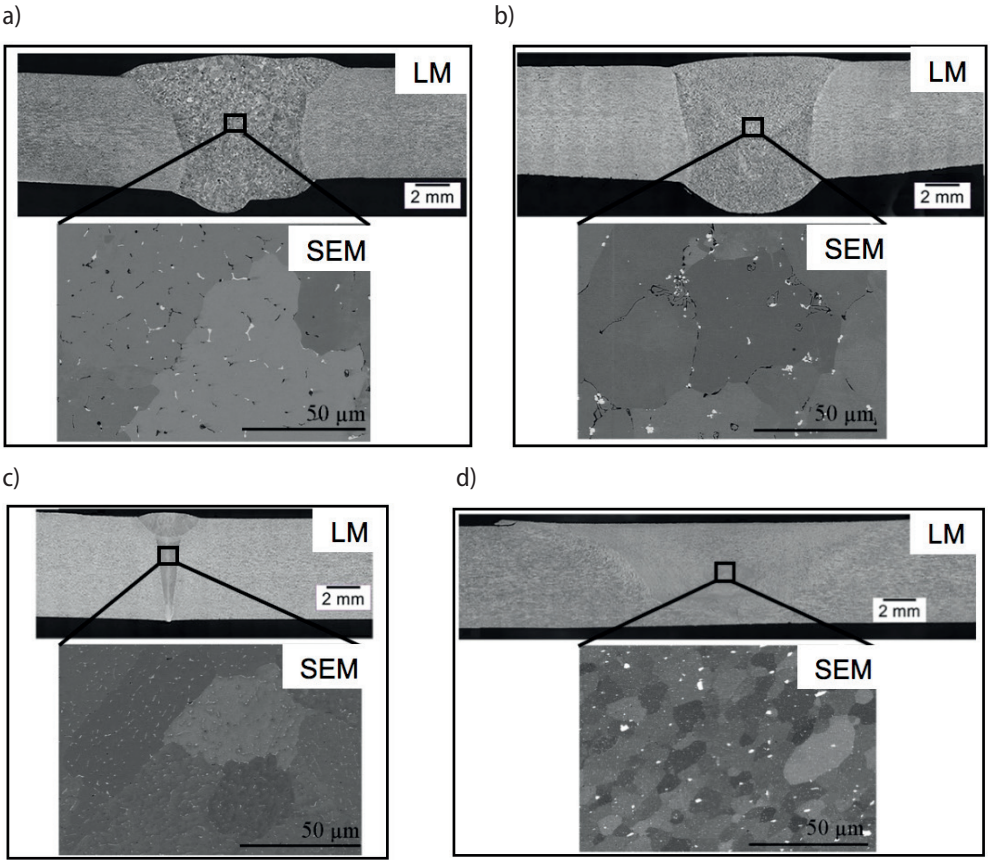

Fig. 2. Microstructure images of welds obtained by light (LM) and scanning electron microscopy (SEM): a) MIG 6082; b) TIG 6082; c) EBW 6082; d) FSW 6082

Figure 3 presents the results of hardness measures of joints. Significant differences in hardness were observed depending on the weld area. In the case of welded joints obtained with the MIG, TIG and FSW methods (Fig. 3a–c), hardness profiles reflect the shape of the "W" letter and are represented by two local minima of about 62 HV. The hardness decrease in these zones, in comparison to the parent material, can be related to the complete or partial dissolution of the strengthening phases after supersaturation and aging, caused by the local increase of temperature during the welding process or/and microstructure recovery and recrystallization, which might occur due to temperature increases in the HAZ. The peak hardness in the area adjacent to the fusion line can be attributed to the phenomenon of solution strengthening and the secondary precipitation of strengthening phases, which decreased along with the distance from the weld. In the area far from the weld, hardness increases and is related to the hardness of parent material.

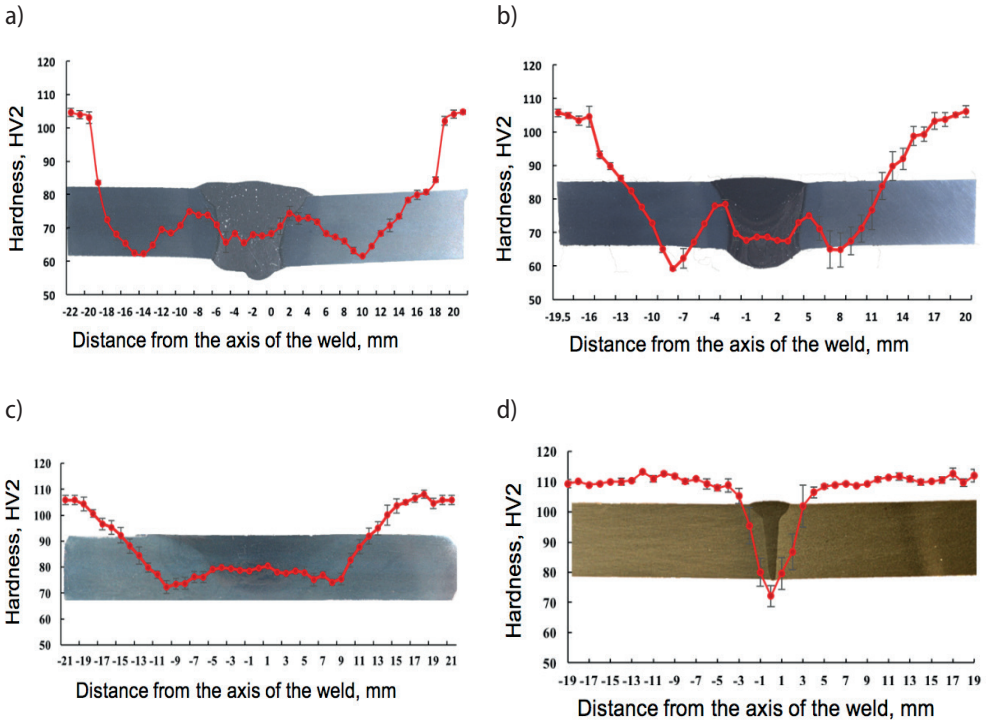

Fig. 3. Hardness distribution in cross-section of joint made with the use of: a) MIG 6082; b) TIG 6082; c) FSW 6082; d) EBW 6082

Similar hardness results were reported in the literature [18]. In the case of the FSW joint, the hardness value is similar across the width of the weld (Fig. 3c) and is 26% lower in comparison to the parent material. The difference in hardness between the welded joint area and the parent material is caused by the effect of deformation and high temperatures during the welding process. The profile and map of the hardness distribution of the EBW 6082 weld are shown in Figure 3d. In comparison to the hardness profiles of joints obtained with the MIG, TIG, and EBW methods, the hardness profile for the EBW joint resembles the letter "V". The center of the weld was characterized by the lowest hardness value of 72 HV. The decrease in hardness by 35% in this area is caused by the dissolution of the strengthening phases (formed as a result of supersaturation and aging) and the formation of the dendritic structure shown in Figure 2c. The average hardness in the HAZ was approx. 90 HV.

The main factor causing structural differences, and consequently changes in the welded joint properties, results from the efficiency of heat supplied by the different welding methods. The influence of the heat input on the welded material is clearly visible in the case of the hardness profiles (Fig. 3). Figure 4 presents the results of mechanical

properties obtained in the uniaxial tensile test. In the case of welded joints obtained with the MIG, TIG, and FSW methods, these properties were similar: the average UTS was about 223 MPa, while the yield strength and total elongation reached values of approximately 172 MPa and 4% respectively. The highest strength properties were obtained in the EBW joint: the average tensile strength was 256 MPa and the yield point was 177 MPa. All samples fractured outside the weld area. On the basis of the UTS values of the welds, the effectiveness of the joints was calculated as the ratio of the joint UTS to UTS of the base material multiplied by 100%. The efficiency of TIG, MIG and FSW joints was calculated to be ~70%, while in the case of the EBW joint, this value was the highest and reached approximately 82%.

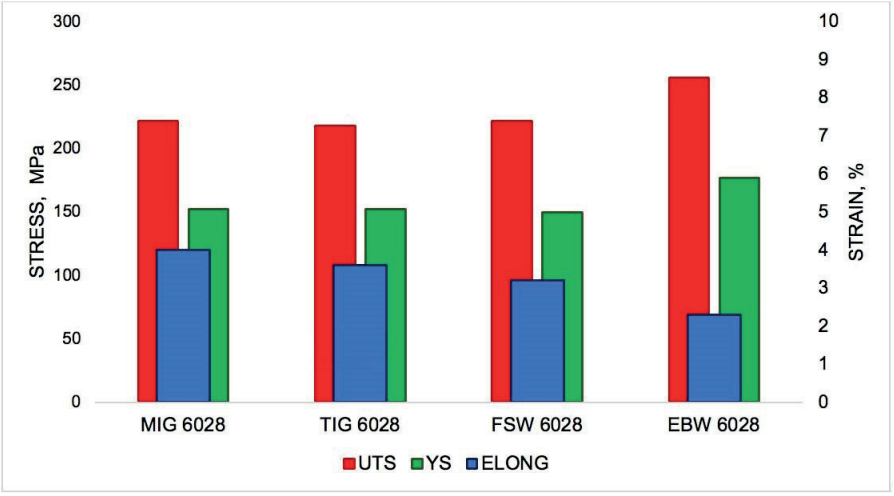

Fig. 4. Mechanical properties of obtained joints obtained under uniaxial tensile test

4. Conclusion

In welds obtained with the MIG, TIG and EBW methods, a dendritic microstructure is developed due to the secondary melting of the parent material or filler.

The applied welding techniques allow homogeneous welded joints to be obtained without imperfections and with similar mechanical properties. The highest joint efficiency for the AA 6082 aluminum alloy was obtained using electron beam welding technology (approx. 82%).

It has been shown that the average hardness of AA 6082 alloy welds in the joint area decreased by about 40 HV units compared to the parent material. Hardness decrease has been associated with the dissolution of strengthening phases and the activation of dynamic recovery and recrystallization processes.

Acknowledgements

Financial support under grant no PBS B5/43/2015, is kindly acknowledged.

References

[1] Noga P., Wiewiora M.: Structural features and mechanical properties of rapidly solidified AlSi alloy. In: METAL 2018: 27th International Conference on Metallurgy and Materials. Brno: TANGER, 2018, 1660–1665
[2] Wloch G., Skrzekut T., Sobota J., Woznicki A., Blaz L.: Sliver matrix composite reinforced by aluminium--silver intermetallic phases. Archives of Metallurgy and Materials, 2017, 62, 427–434
[3] Skrzekut T., Kula A., Blaz L.: Structure evolution in annealed and hot deformed AlMg-CeO_2 composite. Key Engineering Materials, 2016, 682, 259–264
[4] Skrzekut T., Blaz L.: Examination of aluminum matrix composites obtained by powder metalurgy and strenghtened by AgO and CeO_2 particles. In: METAL 2018: 27th International Conference on Metallurgy and Materials. Brno: TANGER, 2018, 1722–1728
[5] Leszczynska-Madej B., Richert M., Wąsik A., Szafron A.: An Analysis of the Microstructure and Selected Properties of the Aluminium Alloys Used in Automotive Air-Conditioning Systems. Metals, 2018, 1–15
[6] Kissel J.R.: Aluminum structures: A guide to their specification and design. Wiley, New York 2002
[7] Birol Y.: The effect of processing and Mn content on the T5 and T6 properties of AA6082 profiles. Journal of Materials Processing Technology, 2006, 173(1), 84–91
[8] Kowalewski Z., Moćko W.: Dynamic Properties of Aluminium Alloys Alloys Used in Automotive Industry. Journal of KONES, 2012, 19, 4–10
[9] Sheppard T.: Extrusion of Aluminium Alloys. Springer, Heidelberg 1999
[10] Greger M., Madaj M., Zacek D.: Structural and mechanical properties of EN AW 6082 aluminum alloy produced by equal-channel angular pressing. Materials and Technologies, 2014, 48(6), 953–958
[11] Williams E.: Light Metals. Springer, Cham 2016
[12] Yibo P., Gang W., Tianxing Z., Shangfeng P., Yiming R.: Dynamic mechanical behaviors of 6082-T6 aluminum alloy. Advances of Mechanicala Engineering, 2013, 5, 1–8
[13] Nowotnik G.M., Sieniawski J., Wierzbińska M.: Influence of long-lasting solution annealing on the microstructure and properties of aluminum alloy 6066. Inżynieria Materiałowa, 2015, 6(6), 381–385
[14] Leśniak D., Woźnicki A., Wojtyna A., Włoch G., Jurczak G.: Effect of hot working temperature and cooling manner during quenching on hardness of 6082 alloy. Rudy i Metale Nieżelazne Recykling, 2016, 61(4), 159–163
[15] Nowotnik G.M., Sieniawski J., Wierzbińska M.: Intermetallic phase particles in 6082 aluminium alloy. Archives of Materials Science and Engineering, 2007, 28(2), 69–76
[16] Wimmer A., Lee J., Schumacher P.: Phase Selection in 6082 Al-Mg-Si Alloys. BHM Berg- und Hüttenmännische Monatshefte, 2012, 157(8–9), 301–305
[17] Nowotnik G.M., Sieniawski J.: Influence of the precipitation strengthening parameters on the microstructure and mechanical properties of AlSi1MgMn alloy. Inżyniera Materiałowa, 2006, 3, 217–220
[18] Svensson L.E., Karlsson L., Larsson H., Karlsson B., Fazzini M., Karlsson J.: Microstructure and mechanical properties of friction stir welded aluminium alloys with special reference to AA 6082. Science and Technology of Welding & Joining, 2000, 5, 285–296